

# Hepatic Radiofrequency Ablation With Internally Cooled Probes: Effect of Coolant Temperature on Lesion Size

Dieter Haemmerich, *Member, IEEE*, Louay Chachati, Andrew S. Wright, David M. Mahvi, Fred T. Lee, Jr., and John G. Webster\*, *Life Fellow, IEEE*

**Abstract**—Radiofrequency (RF) ablation is a minimally invasive method for treatment of primary and metastatic liver tumors. One of the currently commercially available devices employs an internally cooled 17-gauge needle probe. Within the probe, cool water is circulated during ablation, which cools tissue close to the probe resulting in larger lesions. We evaluated the effect of different cooling water temperatures on lesion size. We created a finite-element method model, simulated 12 min impedance-controlled ablation and determined temperature distribution for three water temperatures. Lesion diameters in the model were 33.8, 33.4, and 32.8 mm for water temperatures of 5 °C, 15 °C, and 25 °C, respectively. We solved a simplified model geometry analytically and present dependence of lesion diameter on cooling temperature. We further performed *ex vivo* experiments in fresh bovine liver. We created four lesions for each water temperature, with the same water temperatures as used in the finite-element method (FEM) model. Average lesion diameters were 28.3, 30, and 29.5 mm for water temperatures of 5 °C, 15 °C, and 25 °C, respectively. Water temperature did not have a significant effect on lesion size in the *ex vivo* experiments ( $p = 0.76$ ), the FEM model, and the analytical solution.

**Index Terms**—Ablation, bipolar ablation, finite-element method, hepatic ablation, liver ablation, multiprobe, radiofrequency ablation, RFA, RF ablation.

## I. INTRODUCTION

**R**ADIOFREQUENCY (RF) ablation is a promising, minimally invasive treatment method for primary and metastatic liver tumors. In 2002, an estimated 150 000 new cases of colorectal cancer will be diagnosed in the US alone, with 57 000 deaths [1]. Among men 40 to 79 years old, colorectal cancer is the second leading cause of cancer death. A large number of these deaths are due to liver metastases. In addition, primary liver cancer is one of the most common malignancies worldwide. There were an estimated 437 000 new cases in 1990 with the highest incidences occurring in

Asia and Middle Africa [2]. An estimated 16 600 new cases of primary liver cancer, and over 14 000 deaths will occur in the US in 2002 [1]. Traditionally, the only curative option for patients with liver tumors has been hepatic resection, with a five-year survival between 25% and 60%, compared with a 0% five-year survival without resection [3]–[5]. Unfortunately, only 10%–20% of patients with liver tumors will have disease amenable to surgical resection due to limited hepatic reserve, high surgical risk, or unfavorable tumor location [6], [7]. Currently, clinically used alternative treatments include cryoablation and RF ablation. A recent study of RF ablation in 117 patients has shown 1-, 2- and 3-year survival rates of 93%, 62%, and 41%, respectively [8]. In RF ablation, RF current is delivered to the tissue via electrodes inserted percutaneously, during laparoscopy, or during surgery. The electromagnetic energy is converted to heat by ionic friction. Tissue damage can occur at temperatures above 43 °C with long heating times of several hours [9]; around 3 min of heating time are required at 50 °C. Different modes of controlling the power delivered to tissue are utilized. Power-controlled mode ( $P = \text{constant}$ ), temperature-controlled mode ( $T = \text{constant}$ ) and impedance-controlled mode (power is applied as long as  $Z < \text{constant}$ ) are commonly used. One of the commercially available systems is the Radionics Cool-Tip system (Radionics, Burlington, MA). This system uses 17-gauge needles with active tip exposures of 1, 2, and 3 cm; the remainder of the needle is electrically insulated. Within the probe, water is circulated during the ablation procedure to cool tissue next to the probe and prevent tissue charring [10]. The cooling enables more power to be dissipated in the tissue, resulting in larger lesions of about 2.4-cm diameter compared with 1.2-cm lesion diameter without cooling [11].

We evaluated the effect of changes in temperature of the water used for cooling on lesion size. We created finite-element method (FEM) models of a Cool-Tip probe with 3-cm exposure. We simulated a 12 min, impedance-controlled ablation for different cooling water temperatures of 5 °C, 15 °C, and 25 °C and compared dimensions of the lesions created. We performed an analytical solution of a simplified problem and show change of lesion diameter with temperature. We performed *ex vivo* experiments in bovine liver using the commercial Radionics generator and a Cool-Tip probe with 3-cm exposure. We created lesions while circulating water of 5 °C, 15 °C, and 25 °C temperatures in the probe and compared lesion sizes.

Manuscript received August 5, 2002; revised November 22, 2002. This work was supported by the National Institute of Health (NIH) under Grants HL56413 and DK58839. *Asterisk indicates corresponding author.*

D. Haemmerich, A. S. Wright, and D. M. Mahvi are with the Department of Surgery, University of Wisconsin, Madison, WI 53792 USA.

L. Chachati is with the Department of Electrical & Electronics Engineering, University of Aleppo, Aleppo, Syria.

F. T. Lee, Jr. is with the Department of Radiology, University of Wisconsin, Madison, WI 53792 USA.

\*J. G. Webster is with the Department of Biomedical Engineering, University of Wisconsin, 1550 Engineering Drive, Madison, WI 53706 USA (e-mail: webster@engr.wisc.edu).

Digital Object Identifier 10.1109/TBME.2003.809488

TABLE I  
MATERIAL PROPERTIES USED IN FEM. FOR ELECTRICAL CONDUCTIVITY OF LIVER TISSUE A TEMPERATURE COEFFICIENT OF 2%/°C WAS ASSUMED

Element	Material	$\rho$ [kg/m <sup>3</sup> ]	$c$ [J/kg·K]	$k$ [W/m·K]	$\sigma$ [S/m] (at 25 °C)
Active probe tip	Stainless steel	21500	132	71	4·10 <sup>6</sup>
Probe shaft	Polyurethane	70	1045	0.026	10 <sup>-5</sup>
Tissue	Liver	1060	3600	0.512	0.333

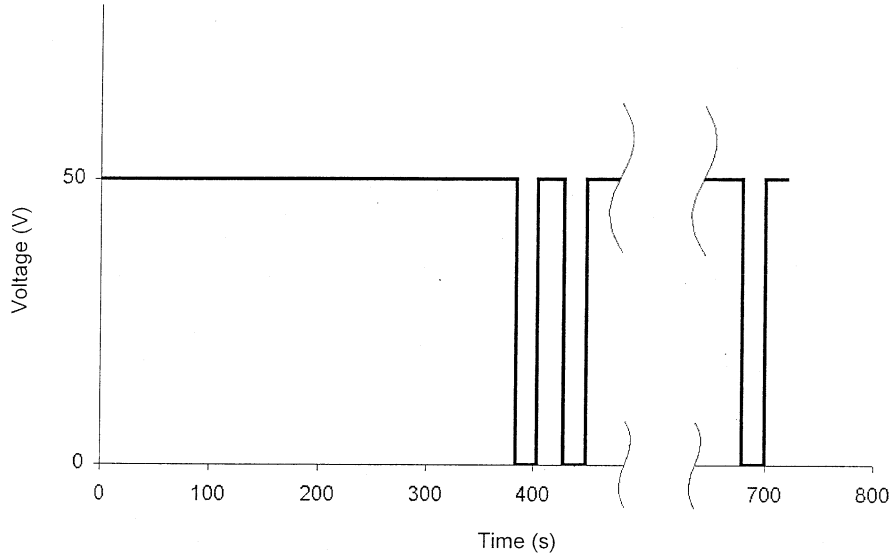


Fig. 1. Applied voltage during impedance-controlled ablation simulation. Voltage was applied until impedance reached threshold, at which point a 20-s cooling period was interleaved.

## II. MATERIALS AND METHODS

### A. FEM Model

Joule heating arises when an electric current passes through a conductor. Electromagnetic energy is converted into heat. The heating of tissue during RF ablation is governed by the bioheat transfer equation [12]

$$\rho c \frac{\partial T}{\partial t} = \nabla \cdot k \nabla T + \mathbf{J} \cdot \mathbf{E} - h_{bl}(T - T_{bl}) - Q_m$$

$$h_{bl} = \rho_{bl} c_{bl} w_{bl} \quad (1)$$

where  $\rho$  is the density (kg/m<sup>3</sup>),  $c$  is the specific heat (J/kg·K), and  $k$  is the thermal conductivity (W/m·K).  $J$  is the current density (A/m<sup>2</sup>) and  $E$  is the electric field intensity (V/m).  $T_{bl}$  is the temperature of blood,  $\rho_{bl}$  is the blood density (kg/m<sup>3</sup>),  $c_{bl}$  is the specific heat of the blood (J/kg·K), and  $w_{bl}$  is the blood perfusion (1/s).  $h_{bl}$  is the convective heat transfer coefficient accounting for the blood perfusion.  $Q_m$  (W/m<sup>3</sup>) is the energy generated by metabolic processes and was neglected since it is small compared with the other terms. Since we compared the simulation results to *ex vivo* experiments, we did not include perfusion in our models.

We created an axisymmetric FEM model for a Cool-Tip probe with 3-cm exposure. The probe was placed within a cylinder of liver tissue (200-mm diameter, 170-mm height). We used the same material properties as previously [13], which are shown in Table I. We used temperature-dependent electrical conductivity, with a temperature coefficient of 2%/°C [14]. If tem-

perature rose above 100 °C, we assumed a rapid drop in tissue conductivity by a factor of 10 000 between 100 °C and 102 °C. This is to emulate vaporization where gas forms and creates an electrically insulating layer. In addition, we applied latent heat associated with water vaporization of 2.257 J/kg, once tissue reached 100 °C. We set the initial temperature of the liver tissue and temperature at the boundary of the model to 25 °C; this is also the initial temperature in the *ex vivo* experiment. We simulated probe cooling by assigning the water temperature (5 °C, 15 °C, or 25 °C) as a boundary condition to the probe, i.e., the probe is kept at constant temperature assuming high water flow rate. We simulated impedance-controlled ablation for 12 min. Constant voltage was applied to the probe throughout the simulation. Dissipated power was 40 W at the start of the simulation and applied voltage was 50 V throughout the whole ablation procedure. Ground potential (0 V) was assigned to the model boundaries. Once impedance rose above the threshold (20  $\Omega$  above baseline value), power was shut down for 20 s, and then reapplied. Fig. 1 shows the alternating scheme of voltage application and 20-s cooling period. This scheme was repeated until the 12 min ablation time was completed. This is an approximation of the actual algorithm used by the Radionics generator [15]. The lesion size was determined using the 50 °C margin (i.e., tissue above 50 °C is considered destroyed). Even though tissue damage is dependent on temperature and time of elevated temperature (i.e., thermal dose) [9], similar lesion dimensions have been predicted by both thermal dose and threshold temperature during ultrasound ablation [16]. In clinical application,

cooling water circulation is turned off at the end of the ablation to fill the lesion gap next to the probe. We did not simulate that in our model since we only measured maximum lesion diameter, which is not affected by the final RF application without cooling. The model consisted of  $\sim 35\,000$  triangular elements and  $\sim 18\,000$  nodes. We used anisotropic mesh. Mesh size was 0.1 mm next to the probe, where high electric and thermal gradients occur, and 1 mm at the model boundaries. We performed convergence tests to ensure that the mesh is sufficiently small. Time steps started at 0.05 s and were automatically controlled so that temperature increase at any node was below 3 °C between steps. We used PATRAN Version 2001 (The MacNeal-Schwendler Co., Los Angeles, CA) to generate the geometric models, assign material properties, assign boundary conditions and perform meshing. We performed a coupled thermo-electrical analysis using the FEM software ABAQUS 6.2 (Hibbit, Karlsson & Sorensen, Inc., Pawtucket, RI). All analysis was performed on a SUN Blade 1000 workstation equipped with 2.5 GB of RAM, and 20-GB hard disk.

### B. Analytical Solution

We determined the steady-state solution to a simplified problem incorporating an ideal conductor of 1.5-mm diameter with infinite length, placed in a tissue cylinder of 200-mm diameter, where we assumed constant thermal and electrical properties. First we solved the electric field problem. We set following electrical boundary conditions:

- ground potential (0 V) at the outer cylinder boundary ( $r = r_1 = 100$  mm);
- potential  $V$  at the conductor, resulting in constant current density  $J(r_0) = J_0$  at the conductor surface ( $r = r_0 = 0.75$  mm).

Due to the cylindrical geometry the current only has a radial component. From the law of charge preservation, the total current through any hypothetical cylinder around the conductor must be constant. Applying this law to the conductor surface ( $r = r_0$ ) and an arbitrary radius ( $r = r_x$ ) yields

$$2\pi r_0 J_0 = 2\pi r_x J_x. \quad (2)$$

We can then express the current at a radius  $r$  as a function of the current at the conductor surface,  $J_0$

$$J(r) = J_0 \cdot \frac{r_0}{r}. \quad (3)$$

The dissipated power density  $p_e$  as a function of radius  $r$  becomes

$$p_e = J \cdot E = \frac{J^2}{\sigma} = \frac{(J_0 \cdot \frac{r_0}{r})^2}{\sigma} = \frac{k_p}{r^2} \quad (4)$$

where  $k_p$  is an arbitrary constant that determines how much power is dissipated.

For the steady-state solution, the left-hand side of the bioheat equation, (1), is equal to zero since  $\partial T / \partial t = 0$ . The steady-state bioheat equation in cylindrical coordinates including the electric power density term from (4) is

$$\frac{k_f}{r} \cdot \frac{\partial}{\partial r} \left( r \cdot \frac{\partial T}{\partial r} \right) + \frac{k_p}{r^2} = 0. \quad (5)$$

We set the following boundary conditions for (5):

- temperature at the outer model boundary  $T(r_1) = T_1 = 25^\circ\text{C}$ ;
- to model probe cooling we set the temperature of conductor surface  $T(r_0) = T_0$ .

The solution for (5) with these boundary conditions is

$$T(r) = \frac{k_p}{k_f} \cdot \left( -\ln^2(r) + \frac{\ln r \cdot (\ln^2 r_0 - \ln^2 r_1) - \ln r_0 \cdot \ln r_1}{\ln \frac{r_0}{r_1}} + \frac{T_0 \cdot \ln \frac{r}{r_1} - T_1 \cdot \ln \frac{r}{r_0}}{\ln \frac{r_0}{r_1}} \right). \quad (6)$$

Since a limitation is that the temperature in the tissue cannot exceed 100 °C, we chose the constant  $k_p$  in a way so that the maximum temperature in the tissue ( $r_0 < r < r_1$ ) is equal to 100 °C. We set the cooling temperature  $T_0$  to 5 °C and 25 °C and show resulting temperature profiles. If no cooling is present, the highest temperatures occur right next to the catheter. We show the result for  $T_0 = 100$  °C assuming no cooling is present. We further performed a parametric study for the dependence of lesion diameter (i.e., 50 °C boundary) on cooling temperature  $T_0$ .

### C. Ex Vivo Experiments

We acquired two pieces of fresh bovine liver from a local butcher. We immersed the tissue in 0.9% saline solution and waited until the liver was at room temperature (25 °C). We placed a Cool-Tip probe with 3-cm exposure into the liver at 5-cm depth. Aluminum foil was located at least 50 cm away from the probe as a dispersive electrode. The ablation probe was perfused with water for cooling. We performed impedance-controlled RF ablation for 12 min, which is the typical time used clinically [15]. We set the maximum power to 40 W, as in the FEM models. In *in vivo* settings, higher power is used; however, since no blood-mediated cooling was present in the *ex vivo* experiment, 40 W was sufficient. We created a total of 12 lesions, four at each different water temperature of 5 °C, 15 °C, and 25 °C in a randomized fashion. The minimum distance between the lesions was 7 cm. After we completed the ablations, we sliced the tissue perpendicular to the direction of probe insertion. We selected the slice where the lesion was largest, and determined average lesion diameter by optical inspection. The boundary between the pale central section and the darker outer section was considered lesion boundary. We performed an analysis of variance (ANOVA) to examine the effect of water temperature on lesion size.

## III. RESULTS

### A. FEM Model

Fig. 2 shows the temperature distribution for a water temperature of 5 °C at the end of the final period of power application (see Fig. 1). Fig. 3 shows the temperature profile versus distance from probe surface for all three water temperatures. The profile was measured at the end of the final period of power application (see Fig. 1). The maximum temperature of  $\sim 102$  °C is reached in the model at a distance of about 2.5 mm from the probe, which is similar to values observed by other investigators

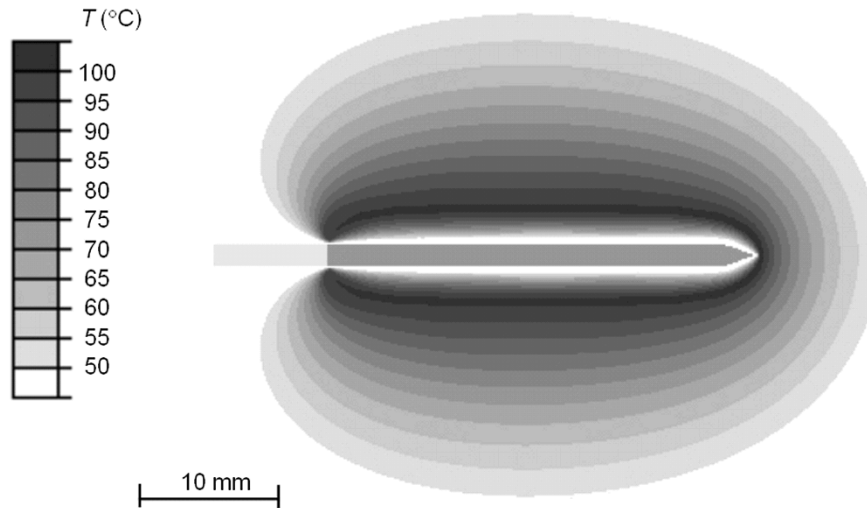


Fig. 2. Temperature distribution after 12 min. ablation for 5 °C water. The outermost border (lightest gray) marks the 50 °C border which is considered lesion boundary. The darker gray portion of the probe represents the active segment.

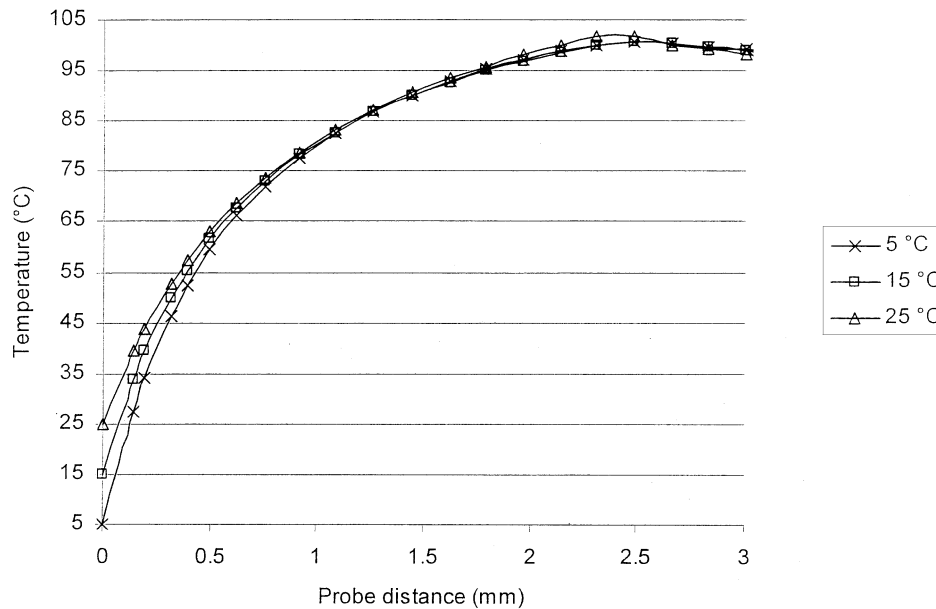


Fig. 3. Temperature profile as function of distance from probe surface. Profile was measured 15 mm from tip, perpendicular to probe surface. Temperature profile is shown for all three different water temperatures. Markers indicate node locations in FEM model.

during *ex vivo* experiments with actively cooled needle probes [17]. Fig. 4 shows the temperature profile at the beginning and at the end of the final cooling period for 5 °C water temperature. All temperature profiles were measured 15 mm from the probe tip. The lesion diameter was 33.8 mm for 5 °C water, 33.4 mm for 15 °C water, and 32.8 mm for 25 °C water. Lesion diameter was measured at the location where it was largest, ~16 mm from the probe tip.

### B. Analytical Solution

Fig. 5 shows the temperature profile of (5) for different cooling temperatures of 5 °C, 25 °C, and 100 °C. Fig. 6 shows the change of lesion diameter with cooling temperature from 0 °C to 100 °C. There is little change in lesion diameter at cooling temperatures below 25 °C. Between 5 °C

and 25 °C cooling temperature, lesion diameter changes by 2.6%, from 131 to 127.6 mm. We can determine the impact of cooling temperature  $T_0$  on the temperature profile  $T(r)$  by examination of (6). The numerator of the right-hand-side term  $T_0 \cdot \ln(r/r_1) - T_1 \cdot \ln(r/r_0)$ , governs the impact of  $T_0$  on  $T(r)$ . At temperatures below 25 °C,  $T_0 \cdot \ln(r/r_1) \ll T_1 \cdot \ln(r/r_0)$ , since  $r_0 \ll r_1$ . Only at high temperatures do we see significant impact, and  $T_0 \cdot \ln(r/r_1) \approx T_1 \cdot \ln(r/r_0)$ .

### C. Ex Vivo Experiments

Fig. 7 shows a typical lesion created with the Cool-Tip probe. Table II summarizes the lesion diameter for the three different water temperatures acquired during the *ex vivo* experiments. The ANOVA analysis did not show significant effect of water temperature on lesion diameter ( $p = 0.76$ ).

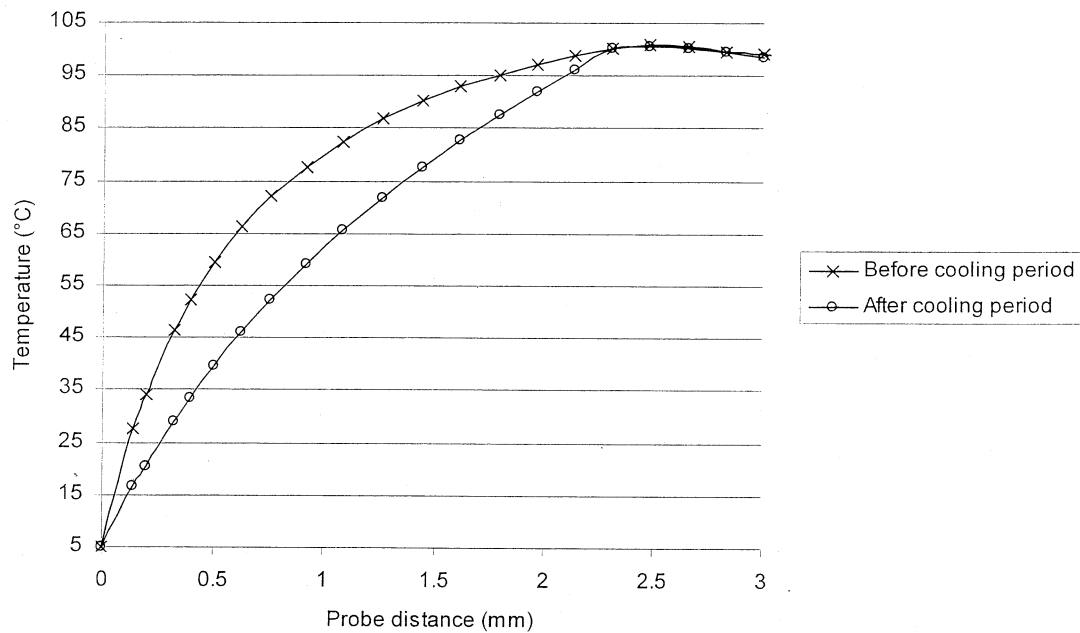


Fig. 4. Temperature profile before and after cooling period for 5 °C water, as a function of distance from probe surface. Profile was measured 15 mm from tip, perpendicular to probe surface. Markers indicate node locations in FEM model.

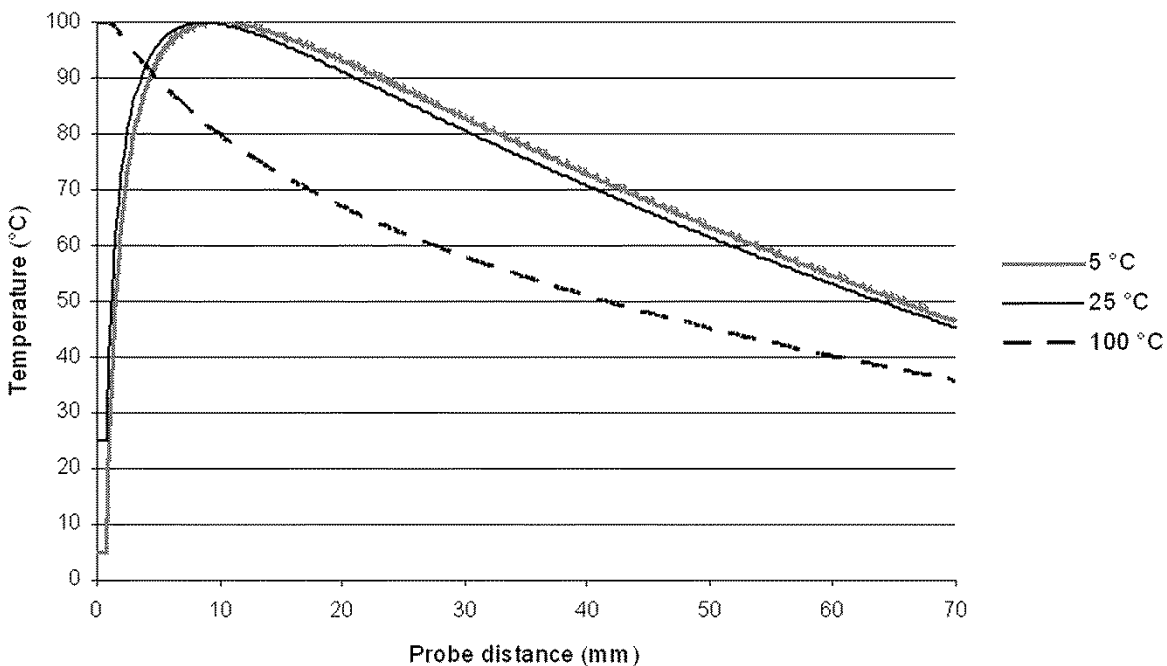


Fig. 5. Temperature profile for analytical steady-state solution of simplified problem.

IV. DISCUSSION

Currently, there are three different systems commercially available in the United States. Rita Medical Systems (Mountain View, CA) and Radio Therapeutics (Sunnyvale, CA) use multiprong probes, whereas Radionics employs a simple needle probe, which is actively cooled internally with water. Rita uses temperature control, Radionics and Radio Therapeutics employ impedance control. The multiprong designs do not utilize active cooling of the probe; heating is greatest next to the probe, which results in tissue charring next to the probe

if temperature rises too high. Tissue charring occurs above 100 °C and creates an electrically highly resistive interface, which impedes further power deposition in the tissue. The charring is irreversible and cannot be removed once it is formed. Active cooling of the probe causes a heat sink effect, which removes heat from the tissue next to the probe. This prevents tissue charring, and enables the deposition of more power into the tissue, thus producing larger lesions than without cooling [11], [17]. Pulsed-power application further increases lesion diameter. Power is applied until impedance reaches a threshold, after which a period of no power application follows

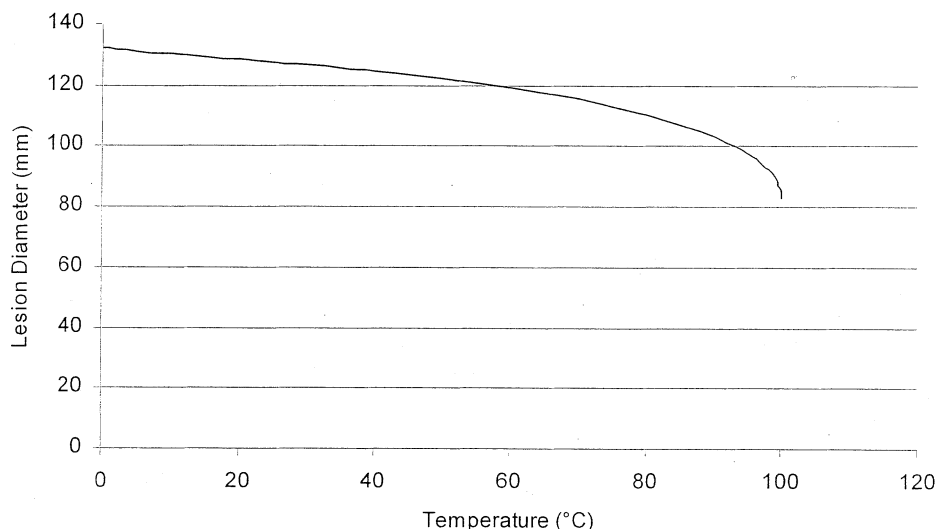


Fig. 6. Analytical solution: lesion diameter vs. cooling temperature.

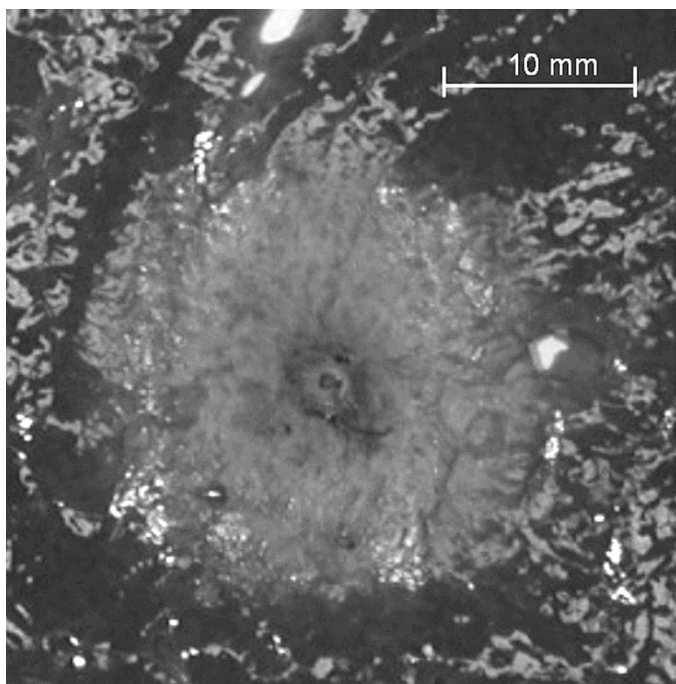


Fig. 7. Cross section of a typical *ex vivo* lesion, 24-mm diameter. The light gray area represents the lesion.

TABLE II  
LESION DIAMETERS FOR *EX VIVO* EXPERIMENTS

	5 °C	15 °C	25 °C
<b>Lesion #1</b>	27 mm	30 mm	27 mm
<b>Lesion #2</b>	24 mm	24 mm	29 mm
<b>Lesion #3</b>	32 mm	32 mm	32 mm
<b>Lesion #4</b>	30 mm	34 mm	30 mm
<b>Average</b>	28.3 mm	30 mm	29.5 mm
<b>StdDev</b>	3 mm	3.7 mm	1.8 mm

(see Fig. 1). This results in preferentially cooling of the tissue close to the probe, but negligible cooling of the tissue near the lesion boundary (see Fig. 4). At distances greater than 2.5 mm

from the probe surface the tissue temperatures before and after the cooling period are virtually the same. Note however, that perfusion is not included in the model and, therefore, the situation likely will be different in the *in vivo* case.

In both the FEM models and the analytical solution, the temperature distribution was similar for all water temperatures between 5 °C and 25 °C. The only notable differences in temperature were seen very close to the probe (see Fig. 3). Close to the probe, the tissue temperature difference between the different water temperatures is highest. However, already at 1 mm from the probe surface the temperature is almost the same for all three water temperatures, lying within a range of 82.5 °C to 83.3 °C for the different water temperatures. Subsequently, the location of maximum temperature is also similar for all water temperatures. During RF ablation, only tissue close to the probe is heated directly by the RF current. The lesion then propagates by thermal conduction until an equilibrium is reached (i.e., the lesion cannot grow beyond a certain size). For a probe without cooling, maximum heating occurs right next to the probe since this is the location of largest current density, and the lesion is mainly formed by thermal conduction (see Fig. 5). Current density is highest close to the probe, most pronounced at the tip and at the interface between exposed and insulated portions of the probe.

When we cool the probe, we create a heat sink that cools the tissue in the probe vicinity. The location of maximum temperature is shifted about 2.5 mm away from the probe surface (see Figs. 2 and 3). Beyond this point of maximum temperature, the lesion is mainly formed passively by thermal conduction. The lower the cooling temperature, the larger region we are able to cool. Since the tissue also acts as a thermal insulator, there is a limit on the region we can cool with a heat sink by thermal conduction. Apparently, at cooling temperatures of 5 °C to 25 °C we already are in the limiting region, and as a result we observe little difference in lesion size when we lower the cooling temperature.

Intuitively, a lower temperature of the cooling water should result in a larger lesion due to an increased heat sink effect of

cooling next to the probe. However, the analytical solution, the FEM model as well as the *ex vivo* experiments show no significant increase in lesion diameter with lower water temperature. The increase in lesion diameter was 2.6% in the analytical solution and 3% in the FEM model when the water temperature was lowered from 25 °C to 5 °C. The *ex vivo* experiments did not show significant difference in lesion diameter ( $p = 0.76$ ) and support the model results. The models correctly predicted that this intuitively obvious method of enhancing lesion size is not effective.

The lesion diameter resulting from the analytical model is much larger (135 mm) compared with the FEM model (33.3 mm) and *ex vivo* results (29.3 mm). This is mainly due to the simplified geometry with a probe of infinite length, and due to the steady-state solution which would correspond to applying RF energy for infinite time.

The lesion dimensions predicted by the FEM models (33.3 mm) were 14% larger than measured during the *ex vivo* experiments (29.3 mm). We explain this discrepancy by limitations of the model. Unlike our simplified FEM model, the liver is a very complex electrical and thermal organ due to its inhomogeneity. It is composed of three different types of blood vessels (hepatic arteries, portal veins, hepatic veins) of different diameters and flow velocities, liver parenchyma, hepatic tumors, bile ducts, and stroma, all of which have unique electrical and thermal properties. We did not include change of thermal tissue properties with temperature due to lack of available data. Tungjitkusolmun *et al.* showed the error in lesion volume prediction to be 3.5% when temperature dependence of either thermal conductivity or heat capacity during cardiac RF ablation is neglected [18]. These limitations of our model may lead to inaccurate results.

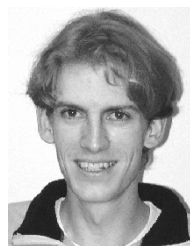
## V. CONCLUSION

The temperature of the water employed for cooling does not significantly affect the lesion size within the range of 5 °C to 25 °C. This conclusion is supported by computer simulations incorporating FEM models, an analytical solution, and *ex vivo* experiments.

## REFERENCES

- [1] A. Jemal, A. Thomas, T. Murray, and M. Thun, "Cancer statistics, 2002," *CA Cancer J. Clin.*, vol. 52, pp. 23–47, 2002.
- [2] F. X. Bosch, J. Ribes, and J. Borrás, "Epidemiology of primary liver cancer," *Sem. Liver Dis.*, vol. 19, pp. 271–285, 1999.
- [3] Y. Fong, J. Fortner, R. L. Sun, M. F. Brennan, and L. H. Blumgart, "Clinical score for predicting recurrence after hepatic resection for metastatic colorectal cancer: Analysis of 1001 consecutive cases," *Ann. Surg.*, pp. 309–318, discussion 318–321, 1999.
- [4] S. S. Yoon and K. K. Tanabe, "Surgical treatment and other regional treatments for colorectal cancer liver metastases," *Oncologist*, vol. 4, pp. 197–208, 1999.
- [5] R. Poon, S. T. Fan, C. M. Lo, I. O. Ng, C. L. Liu, C. M. Lam, and J. Wong, "Improving survival results after resection of hepatocellular carcinoma: A prospective study of 377 patients over 10 years," *Ann. Surg.*, vol. 34, pp. 63–70, 2001.
- [6] R. L. Jamison, J. H. Donohue, D. M. Nagorney, C. B. Rosen, W. S. Harmsen, and D. M. Ilstrup, "Hepatic resection for metastatic colorectal cancer results in cure for some patients," *Arch. Surg.*, vol. 132, pp. 505–510, 1997.

- [7] C. Cha, F. T. Lee, Jr, L. F. Rikkers, J. E. Niederhuber, B. T. Nguyen, and D. M. Mahvi, "Rationale for the combination of cryoablation with surgical resection of hepatic tumors," *J. Gastrointestinal Surg.*, vol. 5, pp. 206–213, 2001.
- [8] L. Solbiati, T. Livraghi, S. N. Goldberg, T. Ierace, F. Meloni, M. Dellanoce, L. Cova, E. F. Halpern, and G. S. Gazelle, "Percutaneous radiofrequency ablation of hepatic metastases from colorectal cancer: Long-term results in 117 patients," *Radiology*, vol. 221, pp. 159–166, 2001.
- [9] S. A. Sapareto and W. C. Dewey, "Thermal dose determination in cancer therapy," *Int. J. Radiat. Oncol. Biol. Phys.*, vol. 10, pp. 787–800, 1984.
- [10] L. Solbiati, S. N. Goldberg, T. Ierace, T. Livraghi, F. Meloni, M. Dellanoce, S. Sironi, and G. S. Gazelle, "Hepatic metastases: Percutaneous radiofrequency ablation with cooled-tip electrodes," *Radiology*, vol. 205, pp. 367–373, 1997.
- [11] S. N. Goldberg, G. S. Gazelle, L. Solbiati, W. J. Rittman, and P. R. Mueller, "Radiofrequency tissue ablation: Increased lesion diameter with a perfusion electrode," *Acad. Radiol.*, vol. 3, pp. 636–644, 1996.
- [12] H. H. Pennes, "Analysis of tissue and arterial blood temperatures in the resting human forearm. 1948," *J. Appl. Physiol.*, vol. 1, pp. 93–122, 1948.
- [13] D. Haemmerich, S. T. Staelin, S. Tungjitkusolmun, F. T. Lee, Jr, D. M. Mahvi, and J. G. Webster, "Hepatic bipolar radio-frequency ablation between separated multiprong electrodes," *IEEE Trans. Biomed. Eng.*, vol. 48, pp. 1145–1152, Oct. 2001.
- [14] K. R. Foster and H. P. Schwan, "Dielectric properties of tissues and biological materials: A critical review," *Crit. Rev. Biomed. Eng.*, vol. 17, pp. 25–104, 1989.
- [15] J. P. McGahan and G. D. Dodd, "Radio frequency ablation of the liver: Current status," *Amer. J. Roentgenol.*, vol. 176, pp. 3–16, 2001.
- [16] S. J. Graham, L. Chen, M. Leitch, R. D. Peters, M. J. Bronskill, F. S. Foster, R. M. Henkelman, and D. B. Plewes, "Quantifying tissue damage due to focused ultrasound heating observed by MRI," *Magn. Reson. Med.*, vol. 41, pp. 321–328, 1999.
- [17] T. Lorentzen, "A cooled needle electrode for radiofrequency tissue ablation: Thermodynamic aspects of improved performance compared with conventional needle design," *Acad. Radiol.*, vol. 3, pp. 556–563, 1996.
- [18] S. Tungjitkusolmun, E. J. Woo, H. Cao, J. Z. Tsai, V. R. Vorperian, and J. G. Webster, "Thermal-electrical finite element modeling for radio frequency cardiac ablation: Effects of changes in myocardial properties," *Med. Biol. Eng. Comput.*, vol. 38, pp. 562–568, 2000.



**Dieter Haemmerich** (S'00–M'02) was born in Vienna, Austria on May 22, 1971. He received the M.S. degree from the Department of Electrical and Computer Engineering, Technical University of Vienna, Vienna, Austria, in 2000, and the M.S. and Ph.D. degrees from the Department of Biomedical Engineering, University of Wisconsin, Madison, in 2000 and 2001, respectively.

He is currently an Assistant Scientist in the Department of Surgery, University of Wisconsin. His research interests include finite-element analysis of

radio-frequency ablation and tissue impedance measurement.



**Louay Chachati** was born in Syria on February 19, 1961. He received the BSEE degree from the Faculty of Electrical and Electronic Engineering, University of Aleppo, Syria, in 1984, and the Ph.D. degree from the Bioengineering Unit, University of Strathclyde, U.K., in 1991.

He is a member at the Faculty of Electrical and Electronic Engineering, University of Aleppo, Syria, teaching undergraduate and postgraduate courses. He received a Fulbright scholarship (2001–2002) and joined the ablation team in the Department of Biomedical Engineering, University of Wisconsin, Madison. His research interests include electronics, PCB technology, and biomedical instrumentation.



**Andrew Wright** graduated from Williams College, Williamstown, MA, and the University of Louisville School of Medicine, Louisville, KY.

He is currently a resident in General Surgery at the University of Wisconsin Medical School, with a special interest in development of new technologies in the advancement of patient care and medical education. He has recently completed a two-year research fellowship studying liver tumor ablation using both radio-frequency and microwave energy.



**Fred T. Lee, Jr.**, received the BA and M.D. degrees from Boston University, Boston, MA, in 1984 and 1986, respectively.

After serving a residency in diagnostic radiology at The University of Rochester, Rochester, NY, he became a faculty member at the University of Wisconsin. He has been the director of abdominal radiology since 2000. His research interests are in tumor ablation and radiographic contrast materials for the detection of cancer.



**David M. Mahvi** attended the University of Oklahoma, and subsequently received the M.D degree in 1981 from the Medical University of South Carolina, Columbia. He then completed the following post-graduate medical clinical training programs at Duke University, Durham, NC: residency in surgery from 1981–1983; fellowship in immunology 1983–1985; residency in surgery 1985–1989. In 1989, he joined the Section of Surgical Oncology, Department of Surgery at the University of Wisconsin-Madison where he is now Professor of Surgery and chief of

the section. He is also a member, University of Wisconsin Comprehensive Cancer Center.



**John G. Webster** (M'59–SM'69–F'86–LF'97) received the B.E.E. degree from Cornell University, Ithaca, NY, in 1953, and the M.S.E.E. and Ph.D. degrees from the University of Rochester, Rochester, NY, in 1965 and 1967.

He is Professor Emeritus of Biomedical Engineering at the University of Wisconsin-Madison. In the field of medical instrumentation, he teaches undergraduate and graduate courses, and does research on radio-frequency cardiac and hepatic ablation.

He is editor of *Medical Instrumentation: Application and Design, 3rd Ed.* (New York: Wiley, 1998), *Encyclopedia of Electrical and Electronics Engineering* (New York: Wiley, 1999), and *Minimally Invasive Medical Technology* (Bristol, UK: IOP, 2001).

Dr. Webster is the recipient of the 2001 IEEE-EMBS Career Achievement Award.